

# Metabonomic analysis reveals correlations between mycotoxins and secondary metabolites in *Penicillium expansum* cultures via time-of-flight mass spectrometry<sup>☆</sup>

Shunbo Liu<sup>a,b</sup>, Youming Shen<sup>a,\*</sup>, Ning Ma<sup>b,\*</sup>, Shan Jiang<sup>a,b</sup>, Jianyi Zhang<sup>a</sup>, Lixue Kuang<sup>a</sup>, Guofeng Xu<sup>a</sup>

<sup>a</sup> Laboratory of Quality and Safety Risk Assessment for Fruit (Xingcheng) Ministry of Agriculture and Rural Affairs, Quality Inspection and Test Center for Fruit and Nursery Stocks Ministry of Agriculture and Rural Affairs (Xingcheng), Research Institute of Pomology Chinese Academy of Agricultural Sciences, Xingcheng 125100, Liaoning, PR China

<sup>b</sup> College of Veterinary Medicine, Veterinary Biological Technology Innovation Center of Hebei Province, Hebei Agricultural University, PR China

## ARTICLE INFO

### Keywords:

*Penicillium expansum*  
Blue mold  
Mycotoxin  
Metabolite  
Biomarker

## ABSTRACT

*Penicillium expansum* is a major postharvest pathogen causing fruit decay and mycotoxin contamination. This study investigated the mycotoxin production and metabolic profiles of 91 *P. expansum* strains using metabolomic analysis. Six mycotoxins were identified, with patulin (PAT) and chaetoglobosin A being particularly prevalent at 77.56 and 45.58 mg·kg<sup>-1</sup> respectively. Untargeted metabolomics profiled 506 metabolites, revealing a decrease in major metabolites during cultivation due to fungal assimilation. Comparative analysis between high- and low-PAT samples showed distinct metabolic signatures in organic acids, benzenoids, organoheterocyclic metabolites, which are linked to mycotoxin production pathways. These differential metabolites were used to build discriminant models, with random forest model achieving 98 % accuracy in distinguishing high- and low-PAT samples. Metabolites, mainly 3, 4-dihydroxybenzoic acid and 4-ketopimelic acid, were explored as potential biomarkers for PAT contamination diagnosis. This research enhances the understanding of *P. expansum*'s metabolic diversity and supports improved fruit quality and safety control.

## 1. Introduction

Fruits are vital agricultural commodities, providing essential vitamins and bioactive compounds that are critical for human health (Li & Ma, 2024). In recent years, with growing health awareness, global fruit consumption has been rising steadily (Yang et al., 2020). Particularly, in China, fruits have become a leading horticultural product, accounting for nearly 20 % of the total output value of the planting sector (<http://www.fao.org/faostat/en/>). However, fruit postharvest fungal infections cause decay and quality decline, resulting in 20 % to 30 % losses of the total yield (Shen et al., 2021). *Penicillium expansum* (*P. expansum*) is a significant pathogen affecting a diverse range of pome fruits including apple and pear, causing blue mold disease (Wang et al., 2023). Moreover, *P. expansum* produces toxic secondary metabolites known as mycotoxins, which pose serious acute toxicity and potential carcinogenic effects to humans and animals (de Sales-Neto & Rodrigues-

Mascarenhas, 2024; Puel et al., 2010). Therefore, *P. expansum* infection and mycotoxin contamination compromise the quality and safety of fruit products (Chen et al., 2023). Understanding its metabolic traits and mycotoxin production is essential for developing targeted quality control strategies.

*Penicillium* metabolites play a critical role in pharmaceutical research and development. In the early 20th century, Alexander Fleming's discovery of penicillin revolutionized antibacterial research and spurred exploration into *Penicillium*'s secondary metabolites and their diverse biological properties (Choudhary et al., 2022; Meister & Silverberg, 2022). Since then, many secondary metabolites have been identified, highlighting *Penicillium*'s remarkable metabolic diversity (Frisvad et al., 2004; Zhang et al., 2022). While much research on *Penicillium* secondary metabolites has focus on pharmaceutical species, the metabolic profile of the fruit pathogen *P. expansum* remains poorly understood (Li et al., 2023; Maldonado et al., 2022). The effects of these uncharacterized

<sup>☆</sup> This article is part of a Special issue entitled: 'IFPFS 2024' published in Food Chemistry: X.

\* Corresponding authors.

E-mail addresses: [shenyouming@caas.cn](mailto:shenyouming@caas.cn) (Y. Shen), [maning9618@163.com](mailto:maning9618@163.com) (N. Ma).

<https://doi.org/10.1016/j.fochx.2025.102475>

Received 26 January 2025; Received in revised form 24 March 2025; Accepted 15 April 2025

Available online 16 April 2025

2590-1575/© 2025 The Authors. Published by Elsevier Ltd. This is an open access article under the CC BY-NC-ND license (<http://creativecommons.org/licenses/by-nc-nd/4.0/>).

metabolites on fruit safety remain unknown, hindering accurate assessment and evaluation. In-depth research into the metabolic profile of *P. expansum* is critical for enhancing the understanding of its metabolic traits and ensuring fruit quality and safety.

Metabolite analysis requires careful sample preparation and advanced analytical techniques. Traditional methods like liquid chromatography (LC), UV-visible absorption spectrometry, mass spectrometry (MS), and nuclear magnetic resonance are essential for identifying metabolites (Bisht et al., 2021; Nanda et al., 2021; Nolvachai et al., 2023; Wille et al., 2012). Recently, liquid chromatography-mass spectrometry (LC-MS) metabolomics has become a leading high-throughput platform with comprehensive databases, offering high sensitivity and precision in analyzing complex metabolite profiles (Broeckling et al., 2023; Kumar et al., 2024; Zhang et al., 2024). This advanced technology provides valuable insights into metabolite dynamics across diverse biological samples, improving the understanding of metabolic pathways (Kathuria et al., 2024; Singh et al., 2024). Despite these technological advances, research on the metabolite profiles of *P. expansum* in fruits remains inadequate. Previous studies have identified several mycotoxins produced by *P. expansum*, including patulin (PAT), citrinin (CTN) (Perrone & Susca, 2017; Tannous et al., 2018), ochratoxin A (OTA) (Brase et al., 2009), chaetoglobosin A (CGA) (Koul & Singh, 2017; Spadaro et al., 2020), mycophenolic acid (MPA) (Brase et al., 2009; Spadaro et al., 2020), penitrem A (PeA) (Barkai-Golan & Paster, 2008; Spadaro et al., 2020), and roquefortine C (RQC) (Frisvad et al., 2004; Spadaro et al., 2020). However, significant gaps remain in our knowledge of the full spectrum of mycotoxins produced by this pathogen in fruits. This study aims to address these limitations by further exploring the mycotoxin profiles of *P. expansum* in fruits, establishing a robust scientific basis for ensuring food safety and effective quality control.

This study explores the metabolic diversity and mycotoxin production differences among 91 *P. expansum* strains from major apple-producing regions in China. By analyzing their mycotoxin production and metabolite profiles, it identifies differential metabolites between high- and low-PAT samples, which could serve as potential biomarkers for PAT contamination diagnosis. The research enhances the understanding of *P. expansum*'s metabolic diversity and provides a scientific basis for improving fruit product quality and safety control.

## 2. Materials and methods

### 2.1. Fungal isolation and identification

Apple samples with typical blue mold symptoms were collected from 91 cold storage facilities located in China's major apple-growing regions during 2021 and 2022 (Table S1). Each sample consisted of at least six diseased apples, which were carefully packaged and transported to the laboratory within three days (Shen et al., 2024). The affected tissues were collected, cut into approximately 1 mm cubes, and underwent a cleaning process: a 30-s rinse in 75 % ethanol followed by three 30-s rinses with sterile water. After air-drying, the samples were incubated on Potato Dextrose Agar (PDA) medium at 25 °C for 2 to 5 days. The dominant *Penicillium* strains were isolated and purified through multiple rounds of subculturing on PDA to ensure strain purity. The pathogenicity of the *Penicillium* strains was confirmed by fulfilling Koch's postulates via re-inoculation onto apple fruits. Molecular identification was conducted via sequencing three key genes—the internal transcribed spacers (ITS) regions 1–4,  $\beta$  tubulin (BenA), and calmodulin (CaM)—and comparing them to NCBI database sequences (Kordalewska et al., 2015; Shen et al., 2024). Strains identified as *P. expansum* were selected for further analysis. Purified fungal spore suspensions were prepared in 20 % glycerol and stored at −80 °C for long-term preservation.

### 2.2. Sample preparation

*P. expansum* spore suspensions were prepared at a concentration of

$10^5$  units per mL through water dilution. Subsequently, 10  $\mu$ L of the spore suspensions were inoculated onto PDA and then incubated at 25 °C with 85 % humidity in the dark. At the designated time points on the day 4 (4d) and day 8 (8d), all colony tissues were harvested, placed into 5 mL centrifuge tubes, and stored at −20 °C for subsequent processing. For metabolite extraction, 200 mg samples were combined with 1 mL of a solvent mixture containing acetonitrile, methanol, and water in a 2:2:1 ratio (v/v) (Zhang et al., 2024). Homogenization was performed at 800 Hz for 1 min. The homogenized samples were subjected to centrifugation at 14,000  $\times g$  for 10 min at 4 °C. Supernatants were harvested and filtered through a 0.22  $\mu$ m nylon membrane. A total of 500  $\mu$ L of the filtrate was prepared for metabolomic analysis. A quality control (QC) sample was prepared through pooling equal volumes of 10  $\mu$ L from each sample.

### 2.3. Instrument analysis

Metabolomic analyses were performed using a UPLC-Q-TOF-MS platform (Triple TOF 5600, AB SCIEX, USA). Chromatographic separations were performed with using an ACQUITY UPLC HSS T3 column (1.8  $\mu$ m particle size, 2.1 mm  $\times$  50 mm dimensions, Waters). Seven mycotoxins—CGA, CTN, MPA, OTA, PAT, PeA, and RQC—were obtained from Sigma-Aldrich (Buchs, Switzerland) and dissolved in acetonitrile at concentrations of 0.20, 0.20, 2.00, 0.50, 1.00, 0.20, and 0.20 mg·mL<sup>−1</sup>, respectively (Fig. 1). These solutions were subsequently stored at −20 °C. Calibration ranges were set from 20 to 2000  $\mu$ g·L<sup>−1</sup> for CGA, CTN, MPA, PeA, and RQC, and 20–10,000  $\mu$ g·L<sup>−1</sup> for PAT and 5 to 5000  $\mu$ g·L<sup>−1</sup> for OTA, across five intervals (Table S2). The mobile phase was prepared with acetonitrile (A) and a buffer solution containing 0.1 % (v/v) formic acid and 5 mmol·L<sup>−1</sup> ammonium acetate in ultrapure water (B). Nitrogen served as both the carrier and protective gas in the mass spectrometry. For comprehensive metabolite ionization, electron spray ionization (ESI) was employed in both positive (ESI+) and negative (ESI-) ionization modes. Optimal chromatographic conditions and mass spectrometry parameters, ensuring efficient instrumental performance, are detailed in Table S3. Samples were analyzed in random order, with a quality control (QC) sample inserted after every five samples to monitor consistency and accuracy. Metabolic data were acquired with Analyst TF 1.8.1 software and stored in the wiff and scan file formats.

### 2.4. Data analysis

The ProteoWizard software was used to convert raw data from mzXML into a compatible format. Subsequent chromatographic peak extraction and alignment were conducted using SCIEX OS software and the XCMS online platform (<https://xcmsonline.scripps.edu/>). Metabolite identification was achieved by analyzing precursor and product ion spectra and cross-referencing with two databases: the plant natural products database from AB SCIEX (USA) and the proprietary database managed by Shanghai Applied Protein Technology Co., Ltd. in China. Metabolite identification followed MSI guidelines using dual criteria: (1) high-precision mass matching (<10 ppm error with MS/MS verification) and (2) confidence-level scoring (level 0–2, threshold  $\geq 0.7$ ) (Blazenovic et al., 2018). The relative concentrations of metabolites were quantified for each sample and compiled into a matrix within a matrix in Microsoft Excel. Differences in metabolite profiles between samples were analyzed using principal component analysis (PCA), supervised partial least-squares discriminant analysis (PLS-DA), and orthogonal partial least-squares discriminant analysis (OPLS-DA) with SIMCA software (version 14.1) (Sliwinski-Bartel et al., 2021). The variable importance in projection (VIP) value for each metabolite was derived from the fitted OPLS-DA model (Freire et al., 2024). Heat map and correlation analysis were conducted using the genescloud tools, a free online data analysis platform (<https://www.genescloud.cn>). Random forest (RF) and support vector machine (SVM) analyses for biomarker discovery were conducted

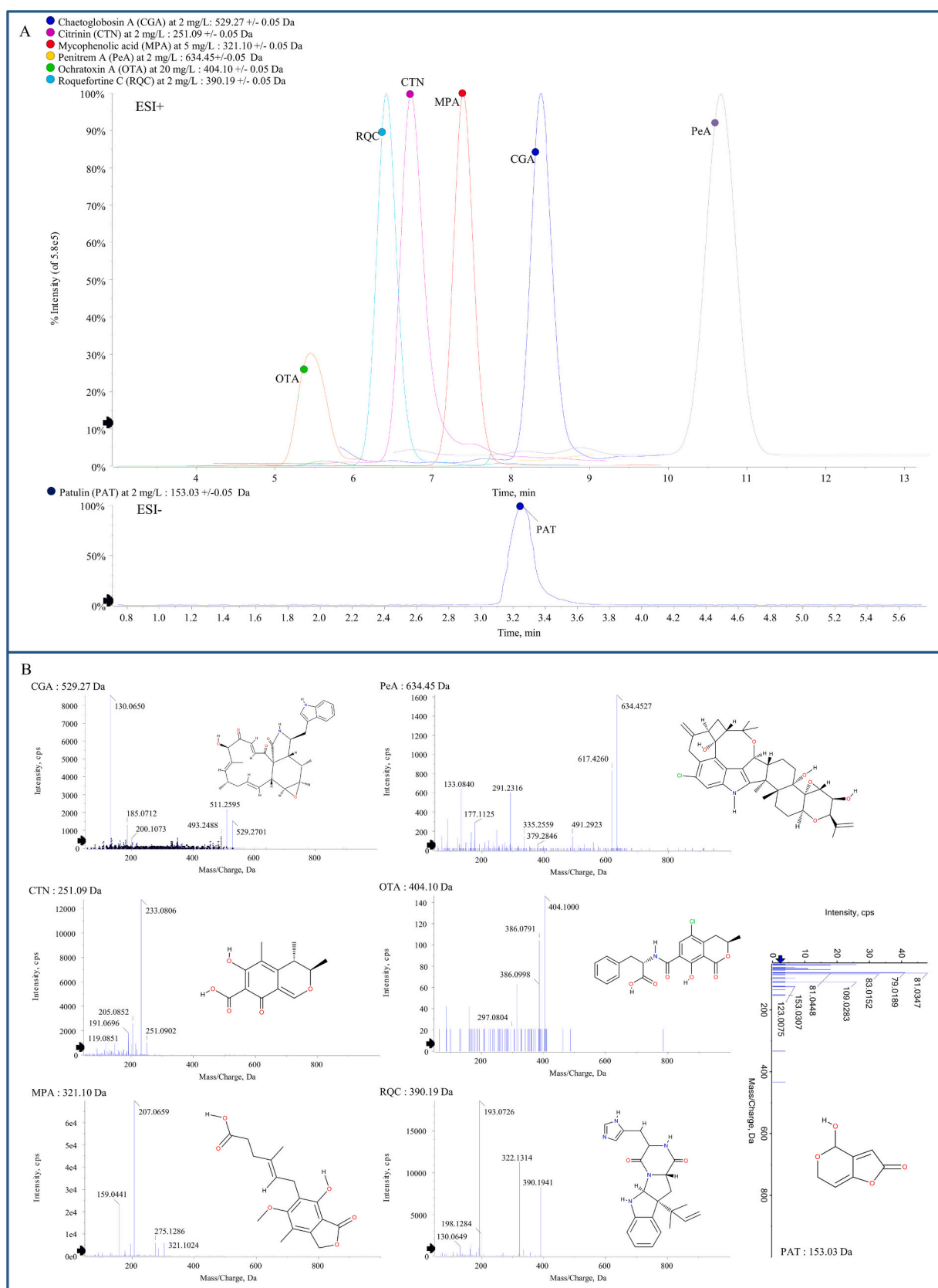


**Fig. 1.** Mycotoxin detection in *Penicillium expansum* cultures. A: Chromatographic profiles of seven mycotoxins: patulin (PAT), citrinin (CTN), ochratoxin A (OTA), chaetoglobosin A (CGA), mycophenolic acid (MPA), penitrem A (PeA), and roquefortine C (RQC). B: Structural representations and mass spectrometric data of the seven mycotoxins.

using the MetaboAnalyst 6.0 online platform (<https://www.metaboanalyst.ca>) (Maione & Barbosa, 2019; Shi et al., 2023). During RF model configuration, three critical hyperparameters, including feature subset size, maximum tree depth, and estimator quantity, were empirically optimized based on cross-validation results. Model performance validation employed receiver operating characteristic (ROC) curve analysis, with the area under curve (AUC) metric serving as the primary indicator of predictive discrimination capability.

### 3. Results

#### 3.1. Fungal identification and analytical method validation

Through systematic process of sample collection, microbial isolation and cultivation, this study obtained 91 pathogenic *P. expansum* strains from major apple-producing regions in China (Table S1). All strains consistently caused characteristic blue mold lesions when re-inoculated on apples. Comprehensive SNP analyses in the ITS, BenA, and CaM genes confirmed these strains as *P. expansum*. These strains were then cultivated on PDA, with samples collected at 4 and 8 days for in-depth metabolite profiling.

The analysis of the QC samples verified the high level of accuracy and stability of the analytical methods. The QC sample was analyzed in 30 replicates across both ESI+ and ESI- modes throughout the entire sample queue. The QC tests consistently generated highly reproducible total ion chromatograms (TICs) in both ionization modes (Fig. S1A-B). Over 81.4 % of positive peaks and 74.2 % of negative peaks exhibited relative standard variation deviation (RSD) values below 30 % (Fig. S1C-D), indicating acceptable variation in peak responses. Multivariate control chart analysis showed that most of QC samples stayed within the three-standard-deviation range (Fig. S2 A). PCA revealed a clear clustering pattern among all QC samples (Fig. S2B). Collectively, these findings confirm the reliability and stability of the analytical methods.

This study developed an analytical method for the simultaneous detection of seven mycotoxins: CGA, CTN, MPA, PAT, PeA, OTA, and RQC. Representative chromatographic and mass spectrometric data (Fig. 1) validate the method's specificity and reliability. The quantitative performance, as demonstrated by linear calibration curves presented in Table S2, exhibits excellent correlation coefficients ( $R^2 > 0.99$ ) for all target analytes, thus establishing robust linear relationships across the tested concentration ranges. This methodological advancement provides a reliable foundation for precise mycotoxin quantification in various samples, improving food safety monitoring and quality control applications.

#### 3.2. Metabolites and mycotoxins identified from fungal cultures

On PDA medium, *P. expansum* strains produce distinctive blue conidia. The colonies exhibited steady growth, with diameters increasing from 1.4 to 2.2 cm on the 4d to 2.7–5.2 cm on the 8d (Fig. 2A). Correspondingly, colony weights increased from 0.10 to 0.68 g on the 4d to 0.25–1.70 g on the 8d (Fig. 2B). The concentrations of six mycotoxins in fungal colonies are shown in Fig. 2C-H. Among these, PAT and CGA had notably higher average concentrations, with average concentrations of 77.56 and 45.58 mg·kg<sup>-1</sup>, respectively. In contrast, the levels of CTN (3.51 mg·kg<sup>-1</sup>), RQC (1.07 mg·kg<sup>-1</sup>), OTA (0.96 mg·kg<sup>-1</sup>), PeA (0.87 mg·kg<sup>-1</sup>) were significantly lower (Fig. 2C-H). MPA was undetectable in any of the analyzed colonies. Statistical analysis revealed higher CTN concentrations in the 8d samples than in the 4d samples (Student's *t*-test,  $p < 0.05$ ). However, the concentrations of other mycotoxins showed no significant differences between 4d and 8d samples.

Comprehensive metabolomic analysis identified 1386 positive-ion and 1033 negative-ion peaks. Metabolite identification analysis characterized a total of 506 metabolites, including 349 positive and 157 negative metabolites. These metabolites represent the comprehensive metabolic profiles of the fungal cultures. The identified metabolites

were classified into several major groups based on their chemical structures: 54 benzenoids, 171 lipids and lipid-like molecules, 97 organic acids and derivatives, 18 organic nitrogen compounds, 34 organic oxygen compounds, 39 organoheterocyclic compounds, 22 phenylpropanoids and polyketides, and 71 unclassified compounds (Fig. S3 A-H). The 4d samples showed higher levels of lipids and lipid-like molecules, organic acids and derivatives, and benzenoids compared to the 8d samples. This suggests that these metabolites are progressively consumed during fungal proliferation, demonstrating dynamic metabolic changes over time.

Spearman correlation analysis revealed significant associations between mycotoxins and metabolites. A heatmap was generated to visualize correlations between the top 50 metabolites and mycotoxins (Fig. 2I). Notably, strong positive correlations were observed between PAT, CGA, RQC, CTN, PeA with key metabolites, suggesting strong biochemical links (Fig. 2I). Conversely, OTA exhibited significant negative correlations with specific metabolites, such as dethiobiotin and chaetoglobosins, indicating a distinct biochemical antagonism. These findings reveal the intricate interplay between mycotoxins and metabolic pathways in *P. expansum*, shedding light on their biochemical interactions.

#### 3.3. Metabolic profiling during *P. expansum* cultivation

To clarify the metabolic differences between 4d and 8d samples, this study employed multivariate analytical methods, including PCA, PLS-DA and OPLS-DA. Initially, PCA was conducted to reduce the data dimensionality with the identified metabolites. The first principal component (PC1) accounted for 48.0 % of the total variance, and the top five PCs together accounted for 71.0 % of the total variance. The 8d samples showed higher PC1 scores than the 4d samples (Fig. 3A). The significant overlap between 4d and 8d samples suggests PCA's limited ability to capture overall variations between the two groups. During model construction, PLS-DA showed a cumulative R<sup>2</sup>Y value of 97.0 % and a corresponding Q<sup>2</sup> value of 84.7 %, indicating strong predictive performance. The PLS-DA plots effectively distinguished the two groups by their inherent metabolic differences (Fig. 3B). The OPLS-DA model showed R<sup>2</sup>Y values of 94.9 % and cumulative Q<sup>2</sup> values of 82.4 %, respectively. The OPLS-DA models showed strong discriminatory power between 4d and 8d samples (Fig. 3C). The reliability and robustness of the OPLS-DA models were confirmed by permutation tests (Fig. 3D), verifying the model's validity and its ability to accurately differentiate between the two sample groups.

The OPLS-DA analysis revealed 243 metabolites with significant differences between the 4d and 8d samples, using OPLS-DA VIP scores >1 and Student's *t*-test *p*-values <0.05 (Fig. 4A and Table S4). Among these, 231 metabolites exhibited a marked decrease in the 8d samples. These metabolites were primarily categorized into the following groups: lipids and lipid-like molecules (84 out of 171, 84/171), organic acids and derivatives (57/97), organoheterocyclic compounds (20/39), benzenoids (14/54), organic nitrogen compounds (9/18), organic oxygen compounds (7/34), phenylpropanoids and polyketides (7/22), and others (21/71) (Fig. 4A and Table S4). The 8d samples showed a significant increase in 12 metabolites, primarily composed of 4 benzenoids and 4 organoheterocyclic compounds. KEGG pathway analysis of these metabolites revealed substantial changes in metabolic pathways between the samples. Key affected pathways included phenylalanine, tyrosine and tryptophan biosynthesis, nicotinate and nicotinamide metabolism; and the metabolism of linoleic acid, purine and sphingolipid (Fig. 4B). These metabolic shifts are closely associated with *P. expansum*'s assimilation process during cultivation.

#### 3.4. Metabolic profiling of high- and low-PAT samples

To clarify the metabolic distinctions between high- and low-PAT samples, this study conducted a comprehensive analysis using PCA,

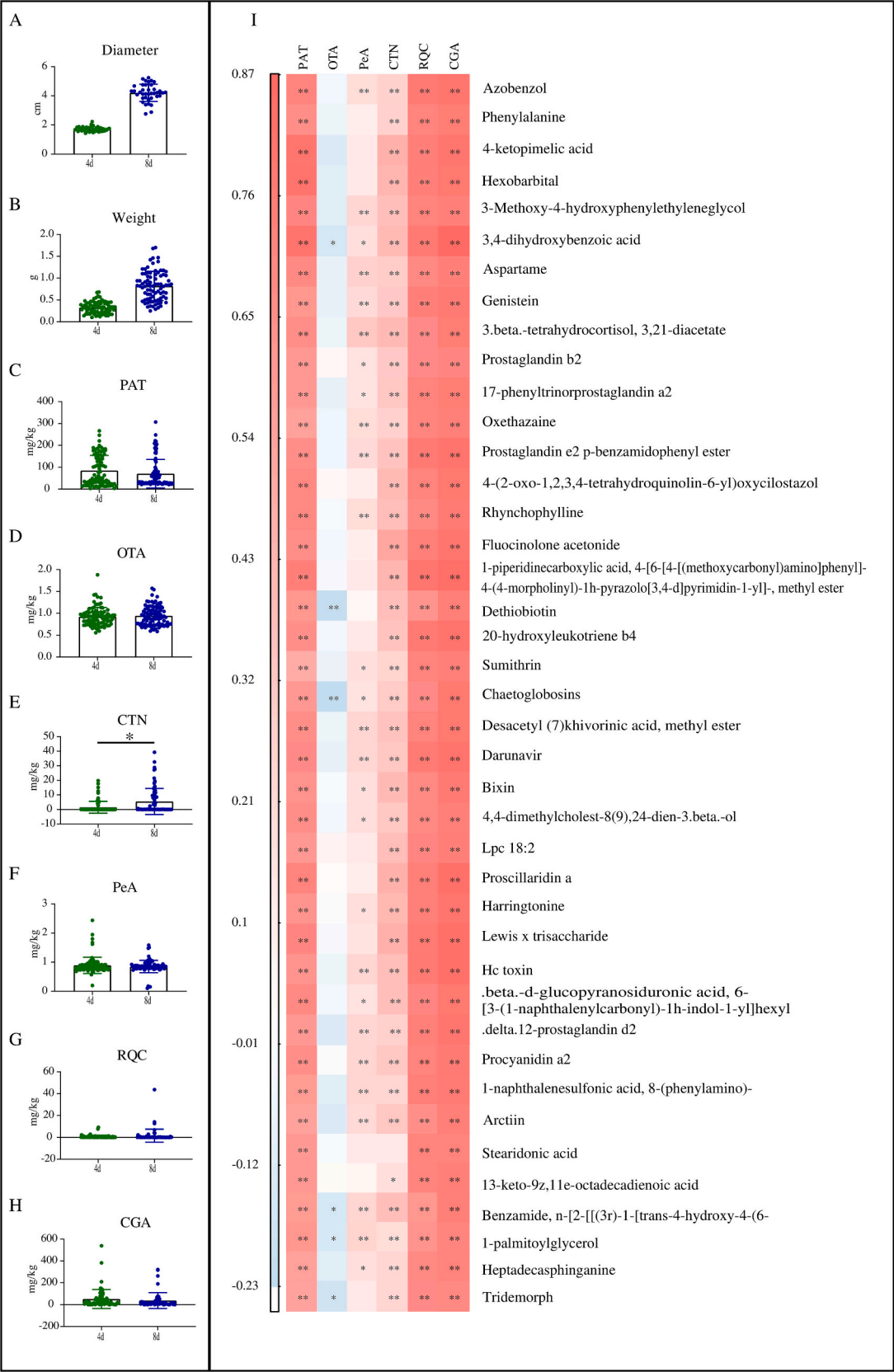


**Fig. 2.** Mycotoxin profiles and their metabolic correlations in 4-day (4d) and 8-day (8d) samples. A-B: Diameters (A) and weights (B) of fungal cultures. C-H: Concentrations of patulin (PAT) (C), citrinin (CTN) (D), ochratoxin A (OTA) (E), chaetoglobosin A (CGA) (F), penitrem A (PeA) (G), and roquefortine C (RQC) (H) in 4d and 8d samples. I: Heatmaps illustrating the correlations between mycotoxins and metabolites (\* $p < 0.05$ , \*\* $p < 0.01$ ).

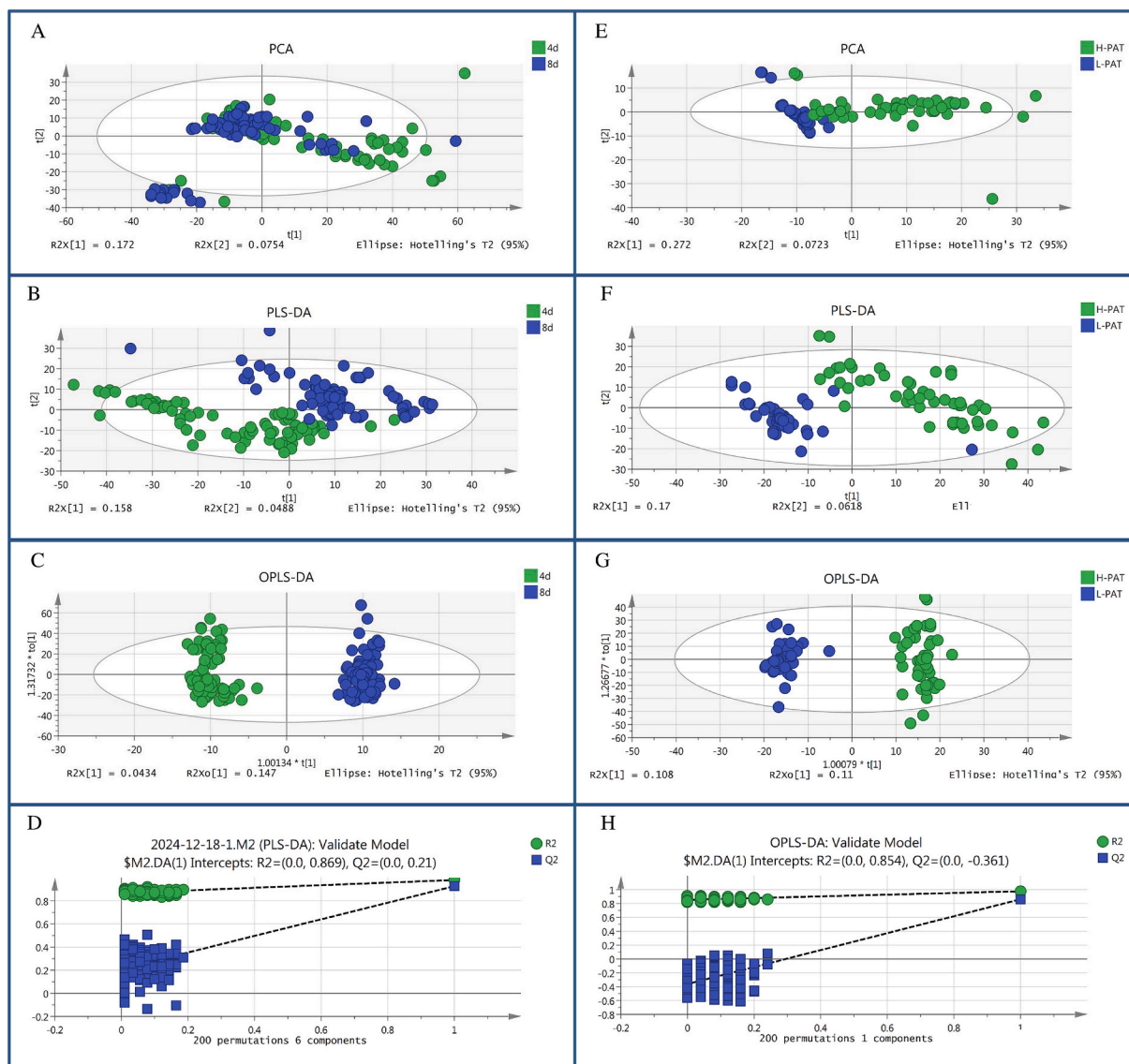


**Fig. 3.** Multivariate statistical analyses, including principal component analysis (PCA), partial least-squares discriminant analysis (PLS-DA), and orthogonal partial least-squares discriminant analysis (OPLS-DA), were conducted to differentiate between various sample groups. A: PCA plot illustrating the separation between 4-day (4d) and 8-day (8d) samples. B: PLS-DA plot demonstrating the discrimination between 4d and 8d samples. C: OPLS-DA plot highlighting the distinction between 4d and 8d samples. D: Permutation tests of the OPLS-DA model between 4d and 8d samples, validating the model's reliability. E: PCA plot showing the differentiation between high-patulin (H-PAT) and low-patulin (L-PAT) samples. F: PLS-DA plot depicting the separation between H-PAT and L-PAT samples. G: OPLS-DA plot emphasizing the distinction between H-PAT and L-PAT samples. H: Permutation tests of the OPLS-DA model between H-PAT and L-PAT samples, confirming the model's robustness.

PLS-DA and OPLS-DA. From the spectrum of PAT concentrations, 100 representative samples were selected for this study: the high-PAT group included 50 samples with PAT concentrations spanning from 108.97 to 306.67 mg/kg, while the low-PAT group included an additional 50 samples with concentrations between 2.84 and 27.83 mg/kg. This selection provided a robust comparison of metabolic profiles across different PAT concentration ranges. Using the identified metabolites, this study performed PCA first to reduce data dimensionality. The first PC accounted for 46.7 % of the total variance, and the top five PCs collectively accounted for 72.1 % of the variance. The unsupervised PCA revealed distinct clustering with clear separation between the high-PAT and low-PAT samples in the two-dimensional plots (Fig. 3E). The high-PAT samples had significantly higher PC1 scores than the low-PAT samples, indicating significant differences in their metabolic profiles. PLS-DA models successfully distinguished high-PAT and low-PAT samples based on their inherent metabolic profiles (Fig. 3F). The PLS-DA

model demonstrated strong predictive performance with a cumulative  $R^2Y$  value of 87.8 % and a  $Q^2$  value of 81.2 % during development. Likewise, OPLS-DA models effectively distinguished between high- and low-PAT samples (Fig. 3G), with  $R^2Y$  and  $Q^2$  values of 96.3 % and 84.8 %, respectively. The reliability and robustness of the OPLS-DA models were confirmed by permutation tests (Fig. 3H).

Through OPLS-DA, 199 metabolites were identified as significant differentiating factors between high-PAT and low-PAT samples, using VIP scores  $>1$  and  $p$ -values  $<0.05$  in Student's  $t$ -test (Fig. 4C and Table S5). These metabolites, primarily elevated in high-PAT samples, were categorized into several classes: organic acids and derivatives (56/97), lipids and lipid-like molecules (43/171), benzenoids (25/54), organoheterocyclic compounds (20/39), organic oxygen compounds (19/34), organic nitrogen compounds (9/18), phenylpropanoids and polyketides (6/22), and other compounds (21/71). KEGG pathway analysis of differential metabolites revealed distinct changes in key

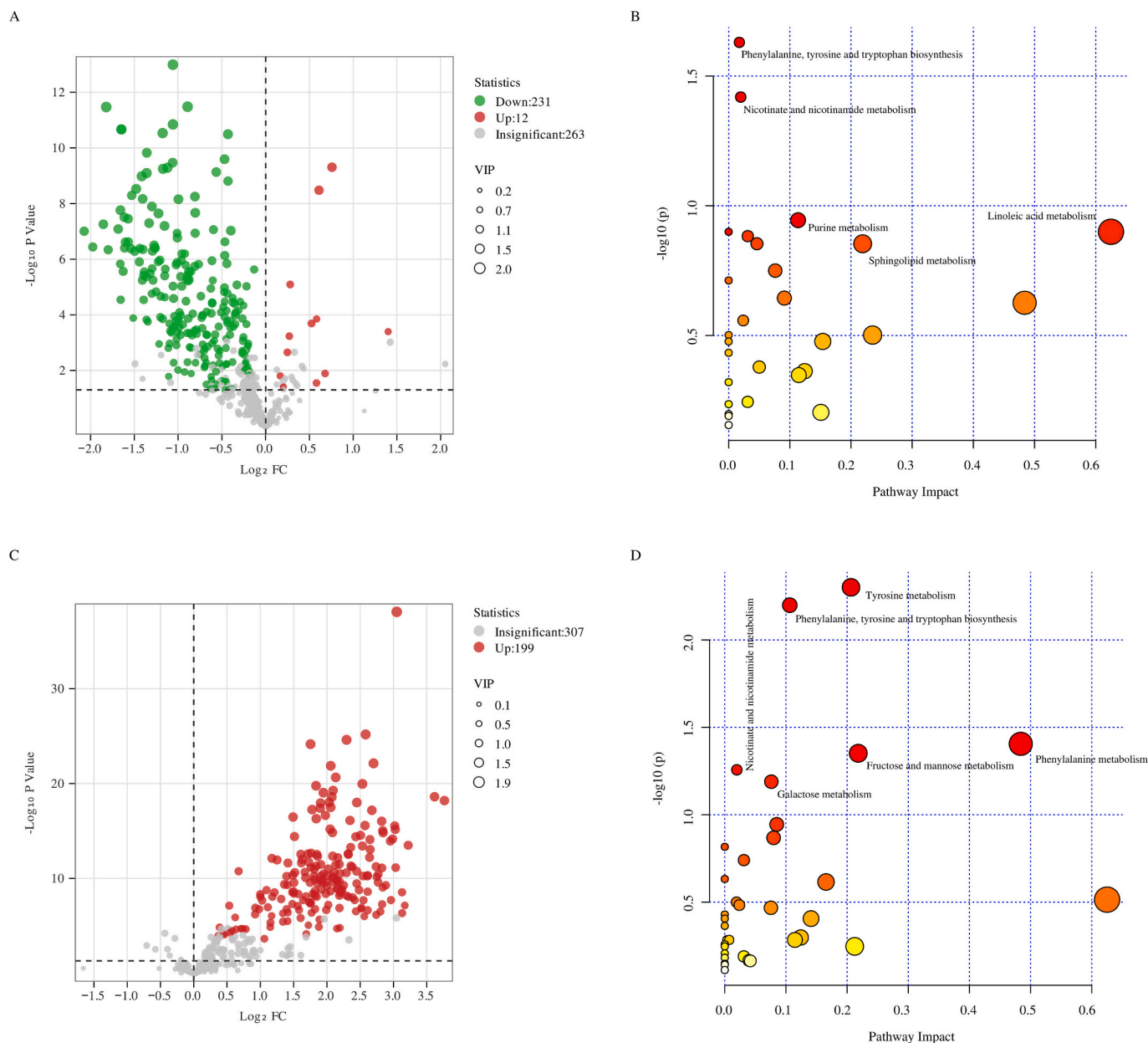


**Fig. 4.** Volcano plots and KEGG pathway analysis of differential metabolites across experimental groups. A: Volcano plots of reflected the change in metabolites between 4-day samples and 8-day samples. B: KEGG analysis reflected the metabolic pathways related to *P. expansum* proliferation. C: Volcano plots of reflected the change in metabolites between high- and low-patulin samples. D: KEGG analysis reflected the metabolic pathway differences between high- and low-patulin samples.

metabolic pathways. The most significantly affected pathways included tyrosine metabolism, phenylalanine, tyrosine and tryptophan biosynthesis, nicotinate and nicotinamide metabolism, fructose and mannose metabolism, as well as phenylalanine and galactose metabolism (Fig. 4D). These pathways were closely linked with the PAT biosynthesis, indicating their potential role in PAT production regulation.

### 3.5. Prediction of PAT level based on fungal metabolites

SVM classification model and ROC analysis were employed to identify potential biomarker. The predictive accuracy of the SVM model ranged from 91.8 % to 96.4 % across different feature sets (5–100), with optimal performance achieved at 15 features (Fig. S4A). Features are selected based on their relative contribution in the classification using cross validation error rates. The top 15 metabolites identified as key features are presented in Fig. 5A. With these features, the SVM model

achieved a classification accuracy of 98.0 % (Fig. 5B). ROC analysis further validated the model's robustness, yielding an area under the curve (AUC) value of 98.3 % (Fig. S4B). Notably, metabolites such as 3, 4-dihydroxybenzoic acid, trihexyphenidyl, 4-ketopimelic acid, and hexaethylene glycol were pivotal in the model construction, underscoring their significance in PAT level prediction.

The RF analysis was employed to establish discriminant models to distinguish high- and low-PAT samples. For optimal performance, the number of features was determined to be 2, the maximum tree depth was set at 7, and the number of estimators was configured as 500 during model construction. The predictive accuracies, assessed with varying numbers of features (5–100), demonstrated a range of 95.5 % to 97.3 % (Fig. S4C). The contribution scores of the top 15 metabolites are depicted in Fig. 5C. The RF model was optimized using these top 15 metabolites, achieving an overall classification rate of 98.0 % (Fig. 5D). ROC analysis further validated the model's performance, demonstrating

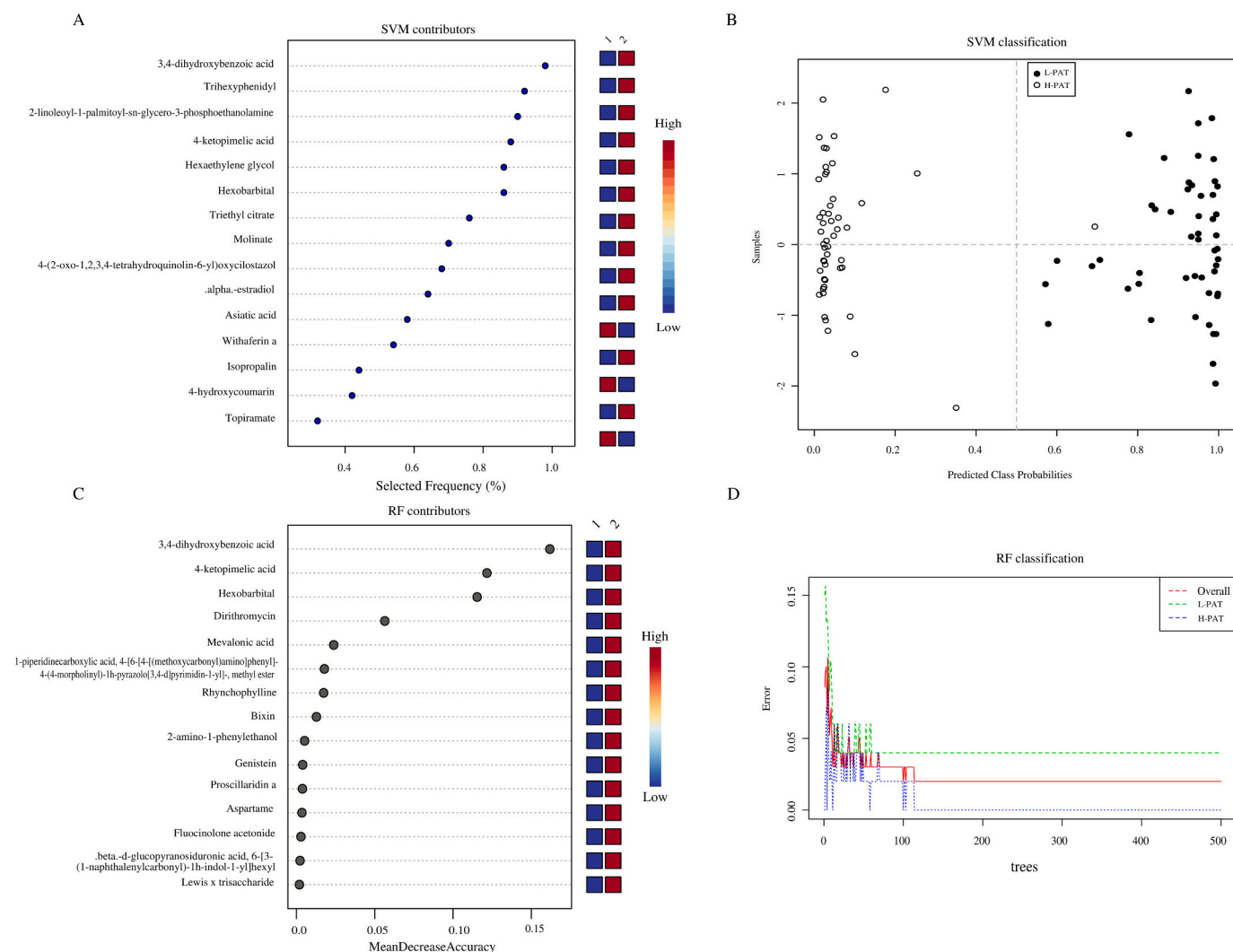


**Fig. 5.** Discrimination of high-patulin (H-PAT) and low-patulin (L-PAT) samples using support vector machine (SVM) and random forest (RF) models. A: Relative importance of the top 15 metabolites utilized in constructing the SVM model. B: SVM classification plots demonstrating the model's ability to distinguish between sample groups. C: Relative importance of the top 15 metabolites employed in the RF model construction. D: Optimized RF decision trees, based on key metabolites, illustrating the stability and robustness of sample classification.

the optimal RF model achieved an AUC of 99.7 % (Fig. S4D). The RF model shows superior discriminative capability for differentiating high- and low-PAT samples. Notably, specific metabolites, such as 3, 4-dihydroxybenzoic acid, 4-ketopimelic acid, and hexobarbital, were consistently identified as significant indicators in both RF and SVM models, highlighting their potential as biomarkers for PAT level assessment.

#### 4. Discussion

*P. expansum* is a prominent pathogenic fungus responsible for post-harvest decay and quality deterioration in fruits (Li et al., 2020). A comprehensive analysis of the mycotoxins and secondary metabolites produced by *P. expansum* is essential for effective manage and assurance the quality and safety of fruit produce (Maldonado et al., 2022; Singh et al., 2024). This study successfully isolated and identified 91 strains of *P. expansum* from primary apple cultivation regions in China. An advanced metabolomics platform using UPLC-Q-TOF-MS was established for comprehensive untargeted metabolite profiling and precise quantification of seven key mycotoxins (Naik et al., 2023). The QC sample analysis demonstrated that the detection method has excellent accuracy and precision, meeting the criteria for reliable and consistent performance (Broeckling et al., 2023; Dunn et al., 2013). This study

provides crucial groundwork for exploring *P. expansum* metabolic diversity and clarifies the correlation between metabolite profiles and mycotoxins, offering insights into *P. expansum* metabolism and toxin biosynthesis mechanisms.

A comprehensive analysis of *P. expansum* cultures revealed the presence of six distinct mycotoxins along with an extensive array of over 500 metabolites, demonstrating the complex metabolic profile of this fungal species. Among these mycotoxins, PAT is the most prevalent contaminant, demonstrating concentrations markedly higher than others; this is consistent with previous research findings (Maldonado et al., 2022). Earlier studies have identified certain toxins such as OTA and CIT in *P. expansum* species (Frisvad et al., 2004; Karlshøj et al., 2007). This study systematically analyzed the mycotoxin profiles of 91 *P. expansum* strains, offering valuable insights and a solid theoretical basis for future research. Notably, CGA concentrations were consistently elevated across most strains. This prevalence highlights the urgent need for enhanced monitoring and further investigation on this toxin's presence in fruit-derived products (Koul & Singh, 2017; Spadaro et al., 2020). This study has successfully characterized 506 distinct metabolites through untargeted metabolomic analysis, presenting a significant advancement in the understanding of the metabolic diversity within *P. expansum*. The method employs a database comparison approach for

metabolite identification, with all metabolite scores surpassing the threshold of 0.7, ensuring high accuracy and reliability (Blazenovic et al., 2018). The heatmap analysis demonstrated distinct correlations between various metabolites and toxins, highlighting significant metabolic interactions between these biological components.

The study compared samples cultured for 4 and 8 days, demonstrating dynamic changes in metabolite and mycotoxin profiles within fungal cultures. Generally, the majority of metabolites exhibited a pronounced decline, likely due to fungal assimilation processes consuming various metabolites. This phenomenon closely resembles the effects of pathogens on fruit composition (Shen et al., 2021; Zhang et al., 2023). Pathogenic infections obtain nutrients from fruits and break down complex macromolecules such as starch and pectin within fruit tissues (Zebeljan et al., 2021; Zhu et al., 2024). Through OPLS-DA analysis, this study successfully identified a range of differential metabolites, predominantly associated with amino acid metabolism, vitamin and cofactor metabolism, and unsaturated fatty acid metabolism pathways (Fig. 4B). The metabolic pathways were identified during initial pathogen-fruit interactions, highlighting their key role in fungal assimilation (Zhang et al., 2023). The content of various mycotoxins remained consistent between the 4d and 8d samples, with the notable exception of CIT, which demonstrated a significantly higher concentration in the 8d sample compared to its 4d counterpart. This is attributed to mycotoxins' unique nature as secondary metabolites that typically do not directly engage in fungi's primary metabolic processes (Li et al., 2020). Notably, as fungal biomass accumulates over time, the absolute concentrations of mycotoxins show a significant increase. This trend highlights the complex mechanisms underlying mycotoxin accumulation.

By comparing differential metabolites between high- and low-PAT samples, this study identified key metabolic pathways associated with toxin biosynthesis and established a basis for predicting toxin concentrations using metabolite profiling. High-PAT samples exhibited significantly higher levels of organic acids and derivatives, which play a role in fungal secretion to acidify the environment and enhance PAT synthesis (Barad et al., 2014; He et al., 2025). Organic acids like gluconic acid can alter the pH, affecting transcription factor PACC activation and pathogenicity factor expression, thereby boosting *P. expansum*'s colonization of host tissue (Barad et al., 2014; He et al., 2025). Additionally, high-PAT samples contained significantly higher levels of benzenoids (25/54) and organoheterocyclic compounds (20/39), which are primarily secondary metabolites potentially linked to toxin synthesis pathways. Pathway enrichment analysis revealed that the predominant pathways associated with these compounds are linked to aromatic amino acid metabolism, particularly tyrosine and phenylalanine metabolism (Fig. 4D), which are likely involved in the biosynthesis of heterocyclic compounds, indicating a pivotal role in the metabolic network (Masuo, 2024). Based on differential metabolites significantly positively correlated with PAT, this study used two machine learning models, SVM and RF, to assess their potential for predicting toxin contamination. Using the selected 15 key metabolites, SVM and RF developed high-resolution discriminative models (with an accuracy of 98 %), with the RF model showing slightly better discriminative performance. These results suggest that nonlinear SVM and RF models, with their multiple parameters and complex calculations, are highly efficient in detecting patterns within intricate datasets (Maione & Barbosa, 2019; Shi et al., 2023). Additionally, several metabolites, such as 3, 4-dihydroxybenzoic acid, 4-ketopimelic acid, and hexobarbital, have been identified as promising biomarkers for predicting PAT levels.

## 5. Conclusion

This study investigated the metabolic diversity and mycotoxin production profiles of 91 *P. expansum* strains through an advanced metabolomic approach with UPLC-Q-TOF-MS. Six distinct mycotoxins were identified from fungal cultures, with PAT and CGA exhibiting elevated levels across most strains, while OTA, CIT PeA, and RQC were

found at lower concentrations. Untargeted metabolomic profiling identified 506 metabolites, with most decreasing during fungal growth, likely attributable to fungal assimilation. Significant metabolic differences were found between high- and low-PAT samples, highlighting distinct biochemical signatures. Using differential metabolites positively correlated with PAT, this study developed predictive models using SVM and RF algorithms, achieving 98 % accuracy in distinguishing between high- and low-PAT samples. Key metabolites, such as 3, 4-dihydroxybenzoic acid and 4-ketopimelic acid, emerged as potential biomarkers of PAT levels. Further validation studies including verification with certified reference materials and practical implementation are required to establish diagnostic reliability and operational consistency of these biomarkers. This research enhances the understanding of *P. expansum* metabolism and supports improved quality and safety control measures for fruit products.

Supplementary data to this article can be found online at <https://doi.org/10.1016/j.fochx.2025.102475>.

## CRediT authorship contribution statement

**Shunbo Liu:** Writing – original draft, Validation, Software, Methodology, Formal analysis, Data curation. **Yuming Shen:** Writing – review & editing, Visualization, Software, Methodology, Investigation, Funding acquisition, Data curation, Conceptualization. **Ning Ma:** Writing – review & editing, Visualization, Supervision, Software, Investigation, Formal analysis, Conceptualization. **Shan Jiang:** Visualization, Methodology, Investigation, Formal analysis. **Jianyi Zhang:** Writing – review & editing, Validation, Methodology, Investigation, Formal analysis, Data curation. **Lixue Kuang:** Writing – review & editing, Validation, Software, Project administration, Methodology. **Guofeng Xu:** Writing – review & editing, Software, Resources, Project administration, Investigation.

## Funding

This work was supported by the Youth Innovation Program of Chinese Academy of Agricultural Sciences (Y2023QC26), the Agricultural Science and Technology Innovation Program (CAAS-ASTIP) and Project of Liaoning Doctoral Research Initiation Fund (2024-BS-303).

## Declaration of competing interest

The authors declare that they have no known competing financial interests or personal relationships that could have appeared to influence the work reported in this paper.

## Data availability

No data was used for the research described in the article.

## References

- Barad, S., Horowitz, S. B., Kobiler, I., Sherman, A., & Prusky, D. (2014). Accumulation of the mycotoxin patulin in the presence of gluconic acid contributes to pathogenicity of *Penicillium expansum*. *Molecular Plant-Microbe Interactions*, 27(1), 66–77. <https://doi.org/10.1094/MPMI-05-13-0138-R>
- Barkai-Golan, R., & Paster, N. (2008). Moldy fruits and vegetables as a source of mycotoxins: Part 1. *World Mycotoxin Journal*, 8(2), 147–159. <https://doi.org/10.3920/WMJ2008.x018>
- Bisht, B., Kumar, V., Gururani, P., Tomar, M. S., Nanda, M., Vlskin, M. S., ... Kurbatova, A. (2021). The potential of nuclear magnetic resonance (NMR) in metabolomics and lipidomics of microalgae- a review. *Archives of Biochemistry and Biophysics*, 710, Article 108987. <https://doi.org/10.1016/j.abb.2021.108987>
- Blazenovic, I., Kind, T., Ji, J., & Fiehn, O. (2018). Software tools and approaches for compound identification of LC-MS/MS data in metabolomics. *Metabolites*, 8(2). <https://doi.org/10.3390/metabo8020031>
- Brase, S., Encinas, A., Keck, J., & Nising, C. F. (2009). Chemistry and biology of mycotoxins and related fungal metabolites. *Chemical Reviews*, 109(9), 3903–3990. <https://doi.org/10.1021/cr050001f>

- Broeckling, C. D., Beger, R. D., Cheng, L. L., Cumeras, R., Cuthbertson, D. J., Dasari, S., ... Mosley, J. D. (2023). Current practices in LC-MS untargeted metabolomics: A scoping review on the use of pooled quality control samples. *Analytical Chemistry*, 95(51), 18645–18654. <https://doi.org/10.1021/acs.analchem.3c02924>
- Chen, Y., Xing, M., Chen, T., Tian, S., & Li, B. (2023). Effects and mechanisms of plant bioactive compounds in preventing fungal spoilage and mycotoxin contamination in postharvest fruits: A review. *Food Chemistry*, 415. <https://doi.org/10.1016/j.foodchem.2023.135787>
- Choudhary, M., Kumar, V., Naik, B., Verma, A., Saris, P. E. J., Kumar, V., & Gupta, S. (2022). Antifungal metabolites, their novel sources, and targets to combat drug resistance. *Frontiers in Microbiology*, 13. <https://doi.org/10.3389/fmicb.2022.1061603>
- Dunn, W. B., Erban, A., Weber, R. J. M., Creek, D. J., Brown, M., Breitling, R., ... Viant, M. R. (2013). Mass appeal: Metabolite identification in mass spectrometry-focused untargeted metabolomics. *Metabolomics*, 9(1), S44–S66. <https://doi.org/10.1007/s11306-012-0434-4>
- Freire, P., Freire, D., & Licon, C. C. (2024). A comprehensive review of machine learning and its application to dairy products. *Critical Reviews in Food Science and Nutrition*. <https://doi.org/10.1080/10408398.2024.2312537>
- Frivstad, J. C., Smedsgaard, J., Larsen, T. O., & Samson, R. A. (2004). Mycotoxins, drugs and other xerotolites produced by species in *Penicillium* subgenus *Penicillium*. *Studies in Mycology*, 49, 201–241.
- He, X., Chen, Y., Tian, S., & Li, B. (2025). PePaA/B/C are required for virulence and patulin biosynthesis by regulating the PePacC-processing proteolytic activity in *Penicillium expansum*. *Food Quality and Safety*, 9. <https://doi.org/10.1093/fqsafe/fyae045>
- Karlshøj, K., Nielsen, P. V., & Larsen, T. O. (2007). Differentiation of closely related fungi by electronic nose analysis. *Journal of Food Science*, 72(6), 187–192. <https://doi.org/10.1111/j.1750-3841.2007.00399.x>
- Kathuria, D., Thakur, S., & Singh, N. (2024). Advances of metabolomic in exploring phenolic compounds diversity in cereal and their health implications. *International Journal of Food Science and Technology*, 59(6), 4213–4233. <https://doi.org/10.1111/ijfs.17056>
- Kordalewska, M., Brillowska-Dąbrowska, A., Jagielski, T., & Dworecka-Kaszak, B. (2015). PCR and real-time PCR assays to detect fungi of *Alternaria alternata* species. *Acta Biochimica Polonica*, 62(4), 707–712. <https://doi.org/10.18388/abp.2015.1112>
- Koul, M., & Singh, S. (2017). *Penicillium* spp.: Prolific producer for harnessing cytotoxic secondary metabolites. *Anti-Cancer Drugs*, 28(1), 11–30. <https://doi.org/10.1097/cad.0000000000000423>
- Kumar, A., Singh, N., & Joshi, R. (2024). Unravelling the metabolomic pool of Ocimum microgreens under diverse growing conditions through targeted compound analysis and non-targeted UHPLC-QToF-IMS based approach. *Food Bioscience*, 59, Article 103984. <https://doi.org/10.1016/j.fbio.2024.103984>
- Li, B., Chen, Y., Zhang, Z., Qin, G., Chen, T., & Tian, S. (2020). Molecular basis and regulation of pathogenicity and patulin biosynthesis in *Penicillium expansum*. *Comprehensive Reviews in Food Science and Food Safety*, 19(6), 3416–3438. <https://doi.org/10.1111/1541-4337.12612>
- Li, C., Zhang, F., Gan, D., Wang, C., Zhou, H., Yin, T., & Cai, L. (2023). Secondary metabolites isolated from *Penicillium expansum* and their chemotaxonomic value. *Biochemical Systematics and Ecology*, 107. <https://doi.org/10.1016/j.bse.2023.104584>
- Li, M., & Ma, S. (2024). A review of healthy role of dietary fiber in modulating chronic diseases. *Food Research International*, 191. <https://doi.org/10.1016/j.foodres.2024.114682>
- Maione, C., & Barbosa, R. M. (2019). Recent applications of multivariate data analysis methods in the authentication of rice and the most analyzed parameters: A review. *Critical Reviews in Food Science and Nutrition*, 59(12), 1868–1879. <https://doi.org/10.1080/10408398.2018.1431763>
- Maldonado, M. L., Patriarca, A., Mc Cargo, P., Iannone, L., Sanchis, V., Nielsen, K. F., & Pinto, V. F. (2022). Diversity and metabolomic characterization of *Penicillium expansum* isolated from apples grown in Argentina and Spain. *Fungal Biology*, 126(9), 547–555. <https://doi.org/10.1016/j.funbio.2022.06.002>
- Masuo, S. (2024). Microbial production of aromatic compounds and synthesis of high-performance bioplastics. *Bioscience Biotechnology and Biochemistry*, 88(11), 1247–1253. <https://doi.org/10.1093/bbb/zbac111>
- Meister, H., & Silverberg, N. (2022). The potential role for phage therapy for genetic modification of cutaneous diseases. *Clinics in Dermatology*, 40(4), 383–387. <https://doi.org/10.1016/j.clindermatol.2022.02.011>
- Naik, B., Kumar, V., Rizwanuddin, S., Chauhan, M., Choudhary, M., Gupta, A. K., ... Rustagi, S. (2023). Genomics, proteomics, and metabolomics approaches to improve abiotic stress tolerance in tomato plant. *International Journal of Molecular Sciences*, 24(3). <https://doi.org/10.3390/ijms24033025>
- Nanda, M., Kumar, V., Arora, N., Vlaskin, M. S., & Tripathi, M. K. (2021). 1H NMR-based metabolomics and lipidomics of microalgae. *Trends in Plant Science*, 26(9), 984–985. <https://doi.org/10.1016/j.tplants.2021.06.004>
- Nolvachai, Y., Amaral, M. S. S., & Marriott, P. J. (2023). Foods and contaminants analysis using multidimensional gas chromatography: An update of recent studies, technology, and applications. *Analytical Chemistry*, 95(1), 238–263. <https://doi.org/10.1021/acs.analchem.2c04680>
- Perrone, G., & Susca, A. (2017). In A. Moretti, & A. Susca (Eds.), 1542. *Penicillium species and their associated mycotoxins* (pp. 107–119). *Mycotoxigenic Fungi: Methods and protocols*.
- Puel, O., Galtier, P., & Oswald, I. P. (2010). Biosynthesis and toxicological effects of patulin. *Toxins (Basel)*, 2(4), 613–631. <https://doi.org/10.3390/toxins2040613>
- de Sales-Neto, J. M., & Rodrigues-Mascarenhas, S. (2024). Immunosuppressive effects of the mycotoxin patulin in macrophages. *Archives of Microbiology*, 206(4). <https://doi.org/10.1007/s00203-024-03928-2>
- Shen, Y., Liu, M., Nie, J., Ma, N., Xu, G., Zhang, J., Li, Y., Li, H., Kuang, L., & Li, Z. (2021). Metabolite changes of apple *Penicillium expansum* infection based on a UPLC-Q-TOF metabolomics approach. *Postharvest Biology and Technology*, 181. <https://doi.org/10.1016/j.postharvbio.2021.111646>
- Shen, Y., Ma, W., Ma, N., Li, M., Zhang, J., & Xu, G. (2024). Genetic identification, pathogenicity and patulin production of *Penicillium* species from apple blue mold in China. *Food Quality and Safety*, 8. <https://doi.org/10.1093/fqsafe/fyad073>
- Shi, S. J., Tang, Z. H., Ma, Y. Y., Cao, C. G., & Jiang, Y. (2023). Application of spectroscopic techniques combined with chemometrics to the authenticity and quality attributes of rice. *Critical Reviews in Food Science and Nutrition*. Early access. <https://doi.org/10.1080/10408398.2023.2284246>
- Singh, N., Kathuria, D., Barthwal, R., & Joshi, R. (2024). Metabolomics of chemical constituents as a tool for understanding the quality of fruits during development and processing operations. *International Journal of Food Science and Technology*, 59(6), 4169–4184. <https://doi.org/10.1111/ijfs.16844>
- Sliwinska-Bartel, M., Burns, D. T., & Elliott, C. (2021). Rice fraud a global problem: A review of analytical tools to detect species, country of origin and adulterations. *Trends in Food Science & Technology*, 116, 36–46. <https://doi.org/10.1016/j.tifs.2021.06.042>
- Spadaro, D., Meloni, G. R., Siciliano, I., Prencipe, S., & Gullino, M. L. (2020). HPLC-MS/MS method for the detection of selected toxic metabolites produced by *Penicillium* spp. in nuts. *Toxins*, 12(5). <https://doi.org/10.3390/toxins12050307>
- Tannous, J., Keller, N. P., Atoui, A., El Khoury, A., Lteif, R., Oswald, I. P., & Puel, O. (2018). Secondary metabolism in *Penicillium expansum*: Emphasis on recent advances in patulin research. *Critical Reviews in Food Science and Nutrition*, 58(12), 2082–2098. <https://doi.org/10.1080/10408398.2017.1305945>
- Wang, K., Ngea, G. L. N., Godana, E. A., Shi, Y., Lanhuang, B., Zhang, X., ... Zhang, H. (2023). Recent advances in *Penicillium expansum* infection mechanisms and current methods in controlling P. *Expansum* in postharvest apples. *Critical Reviews in Food Science and Nutrition*, 63(15), 2598–2611. <https://doi.org/10.1080/10408398.2021.1978384>
- Wille, K., De Brabander, H. F., Vanhaecke, L., De Wulf, E., Van Caeter, P., & Janssen, C. R. (2012). Coupled chromatographic and mass-spectrometric techniques for the analysis of emerging pollutants in the aquatic environment. *TrAC Trends in Analytical Chemistry*, 35, 87–108. <https://doi.org/10.1016/j.trac.2011.12.003>
- Yang, Y., He, D., Wei, L., Wang, S., Chen, L., Luo, M., & Mao, Z. (2020). Association between diet-related knowledge, attitudes, behaviors, and self-rated health in Chinese adult residents: A population-based study. *BMC Public Health*, 20(1). <https://doi.org/10.1186/s12889-020-08896-y>
- Zebeljan, A., Vico, I., Duduk, N., Zibera, B., & Krajnc, A. U. (2021). Profiling changes in primary metabolites and antioxidants during apple fruit decay caused by *Penicillium crustosum*. *Physiological and Molecular Plant Pathology*, 113. <https://doi.org/10.1016/j.pmp.2020.101586>
- Zhang, J., Ma, N., Xu, G., Kuang, L., Li, Z., & Shen, Y. (2023). Metabonomic investigation of *Penicillium expansum* infection of apples and salicylic acid-mediated disease resistance. *Food and Bioprocess Technology*. <https://doi.org/10.1007/s11947-023-03302-y>
- Zhang, J., Ma, N., Xu, G., Kuang, L., & Shen, Y. (2024). Discrimination of apples from the surrounding Bohai Bay and the loess plateau: A combined study of ICP-MS and UPLC-Q-TOF-MS based element and metabolite fingerprints. *Food Chemistry*, 459. <https://doi.org/10.1016/j.foodchem.2024.140279>
- Zhang, X., Yin, Q., Li, X., Liu, X., Lei, H., & Wu, B. (2022). Structures and bioactivities of secondary metabolites from *Penicillium* genus since 2010. *Fitoterapia*, 163, Article 105349. <https://doi.org/10.1016/j.fitote.2022.105349>
- Zhu, Y., Zong, Y., Wang, X., Gong, D., Zhang, X., Zhang, F., Prusky, D., & Bi, Y. (2024). Regulation of sucrose metabolism, sugar transport and pentose phosphate pathway by PacC in apple fruit colonized by *Penicillium expansum*. *Food Chemistry*, 461. <https://doi.org/10.1016/j.foodchem.2024.140863>